SOURCE TERM MODEL FOR STREAMWISE ROD VORTEX GENERATOR MODELLING

Tomasz Kwiatkowski

Institute of Aviation, Department of Aerodynamics
Krakowska Avenue 110/114, 02-256 Warsaw, Poland
e-mail: tomasz.kwiatkowski@ilot.edu.pl

Paweł Flaszyński

The Szewalski Institute of Fluid-Flow Machinery, Polish Academy of Sciences
Department of Aerodynamics
Fiszera Street 14, 80-231 Gdańsk, Poland
e-mail: pawel.flaszynski@imp.gda.pl

Abstract

In the article, the new method of modelling of Rod Vortex Generators (RVGs) was proposed. RVGs are inclined rods, mounted in boundary layer used to flow control. RVGs were intensively investigated in Institute of Fluid-Flow Machinery in Gdansk, Poland. The research results indicate high potential of RVGs to flow control in wide range of Mach numbers (Mach 0.3-1.45) in the main flow. Due to the flow structure details generated by RVG, it is required to create fine grids in the vicinity of RVGs, which increase the computational cost. In order to overcome this difficulty and reduce computational cost the new numerical models of RVGs are proposed, which use the modification of BAY model. Using BAY model it is not needed to resolve the shape of RVG in detail and it is possible to use orthogonal meshes. The BAY model was originally proposed to predict flows behind thin-plate vortex generators. This model works by adding momentum source term to Reynolds-Averaged Navier-Stokes equations in ANSYS Fluent. The BAY model spatial vectors orientation was modified and some simplifications were performed. The model was calibrated and simulations were carried out for the single rod. The results and effectiveness of modified BAY model were compared with wind-tunnel experiment results and grid-resolved model.

Keywords: source term model, rod vortex generator, streamwise vortices, flow control, BAY model, BAY method

1. Introduction

Flow control devices have been widely used on airfoils to control aerodynamic wing loads, separation regions or oscillations of shockwaves [4, 6, 13, 15-17]. The oscillations of shockwave may be harmful due to its high impact on pitching momentum. There are different methods to flow control, in example Gurney flaps [14], jet-vortex generators [5, 9], thin-plate vortex generators [15] or rod-vortex generators, which are considered in this article. Rod vortex generators (RVGs) are newly proposed devices, which were patented by Doerffer, Szwaba and Flaszyński in 2009 [2]. Rod vortex generators (RVGs) are devices that were intensively tested in Institute of Fluid-Flow Machinery in Gdansk, Poland [3, 8, 10-12] due to its high potential to flow control. It can be also effectively applied to control of the shock wave boundary layer interaction effects [7]. RVGs can be successfully use for separation and shock oscillations reduction. In this article, the newly proposed modification of BAY model to predict flow behind RVGs is investigated.

2. Overview of flow setup and implementation of BAY model of rod vortex generator

The dimensions of RVG and its spatial orientation are shown in Fig. 1. The angle of attack was $\theta = 45°$ and angle of incidence was $\Phi = 30°$, the Mach Number in main flow was Ma = 0.3 and the

diameter of RVG was 1 mm and height of RVG was 3.6 mm. The boundary layer height was 10 mm.
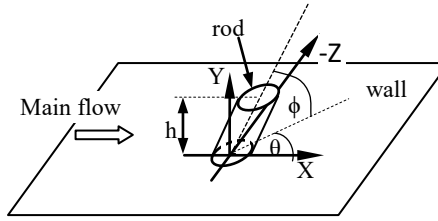

Fig. 1. Schematic of RVG orientation in computational domain [8] (left plot) and

The mechanism of flow control is based on exchange of momentum transfer in the wall-normal direction. The air of high momentum is transferred to the region near wall where is the air of low momentum. The calculations were performed in ANSYS Fluent 14.5 using steady SST k-ω viscous model. Third order MUSCL spatial discretization for convection terms was used with coupled algorithm for pressure-velocity coupling. The extents of computational domain are $X_{min} = -0.025$ m, $X_{max} = 0.08$ m (X is the streamwise coordinate), $Y_{min} = 0$ m and $Y_{max} = 0.05$ m (Y is the wall-normal coordinate), $Z_{min} = -0.032$ m, $Z_{max} = 0.032$ m (Z is the spanwise coordinate). At the main flow inlet was set pressure inlet boundary condition with the profile of total pressure, turbulent kinetic energy and specific dissipation rate to obtain as close flow conditions as used in the experiment. For the computations of BAY model [1] of rod vortex generator BAY method was used, where to the cells encompassing the shape of RVG was added source term using equation (1) of lifting force:

$$\mathbf{L_i} = c_{VG} \, S_{VG} \, \frac{\Delta V_i}{V_m} \alpha \rho \, u^2 \, \mathbf{l}, \tag{1}$$

where:

$\mathbf{L_i}$ – vortex generator source term lifting force,

c_{VG} – relaxation parameter which controls the strength of the side force and consequently the intensity with which the local velocities align with the vortex generator,

S_{VG} – plan-form area of Vortex Generator,

V_i – volume of the cell where the force is calculated,

V_m – the sum of volumes of cells where the force term is applied,

α – the angle of local velocity $\mathbf{u}$ to the vortex generator,

ρ – density of fluid,

$\mathbf{l}$ – unit vector on which the side force acts.

The unit vector $\mathbf{b}$ is the most essential vector defining the orientation of lifting force vector, because it is modelling the $\mathbf{l}$ vector direction as in equation. The $\mathbf{l}$ vector may be modelled using $\mathbf{b}$ vector as in equation (2):

$$\mathbf{l} = \frac{\mathbf{u}}{|\mathbf{u}|} \times \mathbf{b}, \tag{2}$$

where:

$\mathbf{l}$ – unit vector on which the side force acts,

$\mathbf{u}$ – local velocity vector,

$\mathbf{b}$ – unit vector in the direction of lifting force vector.

The unit vector $\mathbf{t}$ is also important of vector used in BAY model and it is approximately oriented in the direction reverse of the main flow, but also in the perpendicular direction to the $\mathbf{b}$ vector. The unit vector $\mathbf{t}$ may be approximated by term (3) which is multiplied with the equation of lifting force $\mathbf{L_i}$ (5):

$$\frac{\mathbf{u} \cdot \mathbf{t}}{|\mathbf{u}|}, \tag{3}$$

where:

u – local velocity vector,
t – unit vector in the direction upwind to the main flow.

The unit vector **n** is the vector product of unit vectors **b** and **t** and is the product of approximation at small angle of attacks originally proposed by Bender et al. (4). In the calculations described in this article the angle of attack α is assumed as 1 in order to reduce computational cost.

$$\alpha = \sin \alpha = \cos\left(\frac{\pi}{2} - \alpha\right) = \frac{\mathbf{u} \cdot \mathbf{n}}{|\mathbf{u}|}, \tag{4}$$

where:

α – the angle of local velocity **u** to the vortex generator,
u – local velocity vector,
n – vector product of unit vectors **b** and **t**.

After taking into account all earlier approximations the final source term equation is given by (5), which is easy to implement in numerical code to calculations.

$$\mathbf{L_i} = c_{VG} \, S_{VG} \, \frac{1}{V_m} \rho \left(\frac{\mathbf{u}}{|\mathbf{u}|} \times \mathbf{b}\right)\left(\frac{\mathbf{u} \cdot \mathbf{t}}{|\mathbf{u}|}\right), \tag{5}$$

where:

L_i – vortex generator source term lifting force,
c_{VG} – relaxation parameter which controls the strength of the side force and consequently the intensity with which the local velocities align with the vortex generator,
S_{VG} – plan-form area of Vortex Generator,
V_m – the sum of volumes of cells where the force term is applied,
ρ – density of fluid,
u – local velocity vector,
b – unit vector in the direction of lifting force vector,
t – unit vector in the direction upwind to the main flow.
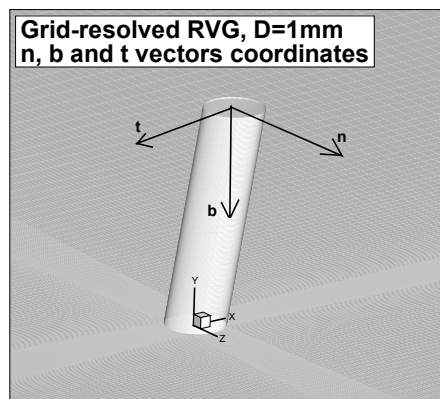

Fig. 2. Spatial orientation of BAY model vectors referenced to rod coordinates

After converged computations of grid-resolved RVG the total force value on the all RVG surfaces was calculated. The X-component of force was 1.49E–2N, the Y component was –3.11E–1N and in the Z direction the component of force was 1.44E–3N. It means that Y component of force contains 99.89% of total force. The surfaces of modelled RVG are presented in Fig. 2 as brightened surfaces. Because the force in Y direction is the most essential, the **b** vector was assumed to orient

with the force in Y direction. At the beginning of calculations the **n** vector was aligned with X Cartesian coordinate vector, but also perpendicular to **b** vector. The **t** vector was orthogonal to vectors **b** and **n**. During numerical calculations, the BAY model vectors were calibrated by rotating around **b** vector and it was observed that the best agreement of plots of circulation was obtained for rotation at angle of 90° around **b** vector from original position. The x, y and z coordinates of **b** vector are $b_x = 0.048845$; $b_y = -0.998806$; $b_z = 0.001274$. The x, y and z coordinates of **t** vector are $t_x = -0.998806$; $t_y = -0.048845$ and $t_z = 0.000062$. The **n** vector of BAY model was not used in order to reduce computational cost.

As shown in Fig. 3 (left) the existence of RVG requires mesh refinement and topology adjustment. If lot of RVGs are investigated, then the mesh become more complex and the simulations are more demanding. The mesh of BAY model contains 920640 cells and it is orthogonal and easy to generate, because there are no any discontinuities in geometry. In Fig. 3 (right) the mesh on lower tunnel wall is presented, where BAY model was used. As shown, this mesh was only refined in the Z direction in the location of vortex in order to resolve the vortex parameters. The mesh with grid-resolved RVG has 6.9 times more cells than mesh used together with BAY model, what influences on increased computational cost.
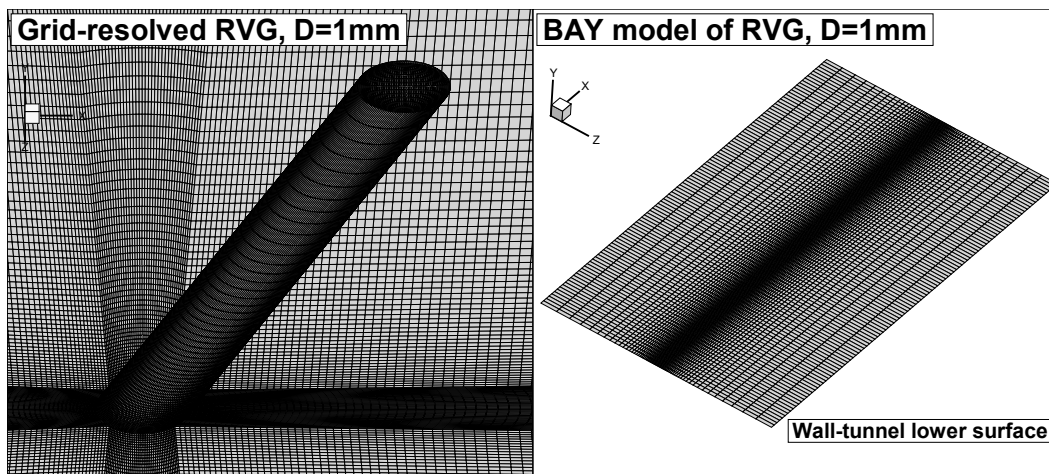

Fig. 3. Comparison of used meshes for computations – the mesh, which resolve the shape of RVG (left figure) and mesh on lower wall-tunnel surface for which the BAY model was used (right figure)

3. Results

In Fig. 4 it is presented comparison of plots of circulation downstream of RVG – grid-resolved RVG and its BAY model calibrated for constant C = 240. Good agreement of plots is obtained, which indicates that BAY model was properly calibrated. Maximum value of circulation is around 0.26 m^2/s. The difference is visible in the region shortly downstream of RVG, from 0 mm to 3 mm. It is caused by different models and vortex creation differences.

In Fig. 5, it is presented the comparison of x-vorticity, static pressure and pathlines for models of grid-resolved RVG in the left plot and its BAY model in the right plot. On the grid-resolved RVG's surface is presented contour of static pressure. In the frontal surface, the static pressure is around 95000 Pa and in the rear part of RVG the static pressure values are around 92600 Pa. The maximum value of static pressure on the surfaces of cells, where source term is added is a bit lower than predicted by grid-resolved RVG and its value is around 94600 Pa. The static pressure on the rear side of cells, where momentum source is added is around 92800 Pa. The pathlines are presented in the region of RVG's vicinity, which generates streamwise vortex. The RVG's presence causes the transport of momentum and energy in the direction normal to the tunnel wall surface. There may be seen 3 vortices at the slice of x-vorticity. The biggest vortex, primary vortex, coloured with red color indicating that this is rotating clockwise it is located near tunnel wall as the effect rod
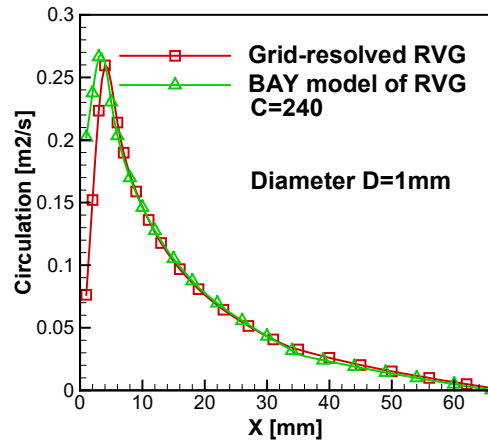
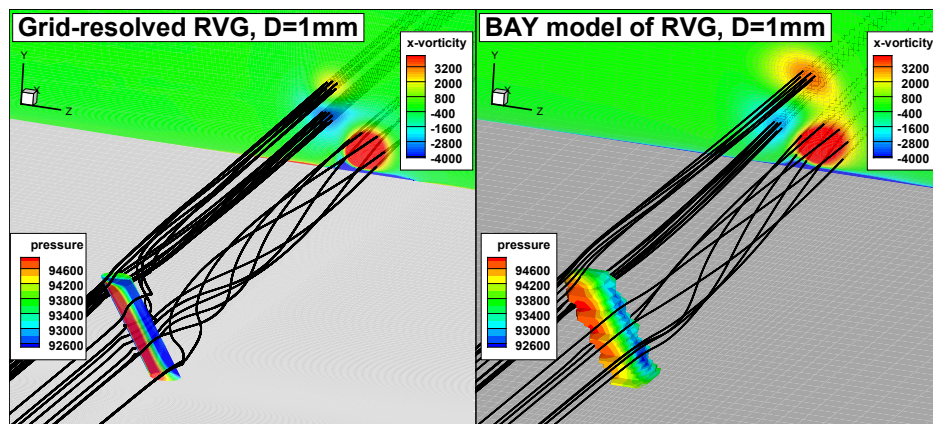*Fig. 4. Plot of circulation behind rod vortex generator placed in X = 0 m*

Fig. 5.   Contour of x-vorticity at slice 4 cm behind RVG with pathlines and static pressure contour on RVG surface (left plot) and on the surfaces of cells, where source term is added in BAY model (right plot)

embedded in the boundary layer. The secondary vortex, coloured by blue colour indicating that this is rotating counter clockwise, is located between clockwise rotating vortices. The second clockwise rotating vortex, the tip vortex, is generated by interaction of main flow with top part of RVG. The similar character of flow is predicted by BAY model of RVG. In the case of BAY model the sizes of primary vortex and smaller tip vortex, both clockwise rotating are a bit larger than vortices predicted by grid-resolved RVG despite of the fact that circulation values are very similar.

Experimental data were also compared with numerical. In Fig. 6, it is presented normalised total pressure (PLocNom), which is referred to the total pressure at corresponding height in wall-normal direction in reference boundary layer non-disturbed by streamwise vortex. As the reference, in the boundary layer outside the region of vortex generator influence of is assumed, which is in this case in $Z = -12$ mm. This shows the local differences in total pressure between the flow with vortex generator and in the reference boundary layer at section located 46 mm downstream of RVG. In the figure, the local minimum and maximum (near the wall surface) of total pressure are shown which indicate the RVG influence on the flow. The differences between minimum and maximum values show the strength of streamwise vortices. The centre of vortex is located between extreme values of total pressure and it is marked by black circle with and arrow indicating the direction of rotation.

In Fig. 7 are presented contours of local normalised total pressure for grid-resolved RVG (left) and BAY model (right) at section 46 mm downstream of RVG, as in the measurement. In the opinion of authors, better agreement of normalised total pressure with measurement is obtained for the case of BAY model of RVG due to similar shape and size of high-pressure regions.
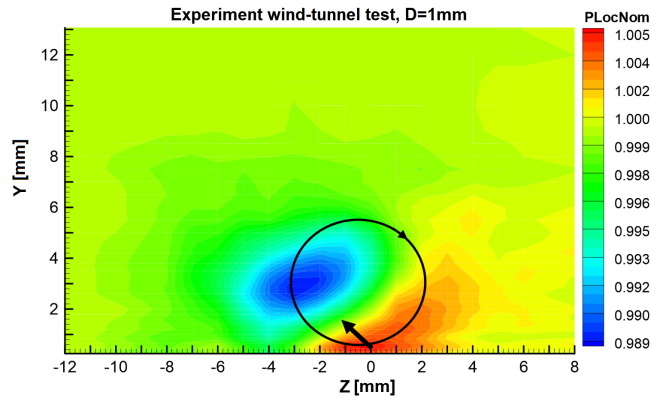
Fig. 6. Normalized local total pressure contour at X = 4.6 cm behind RVG measured in wind-tunnel experiment, diameter D = 1 mm [8]

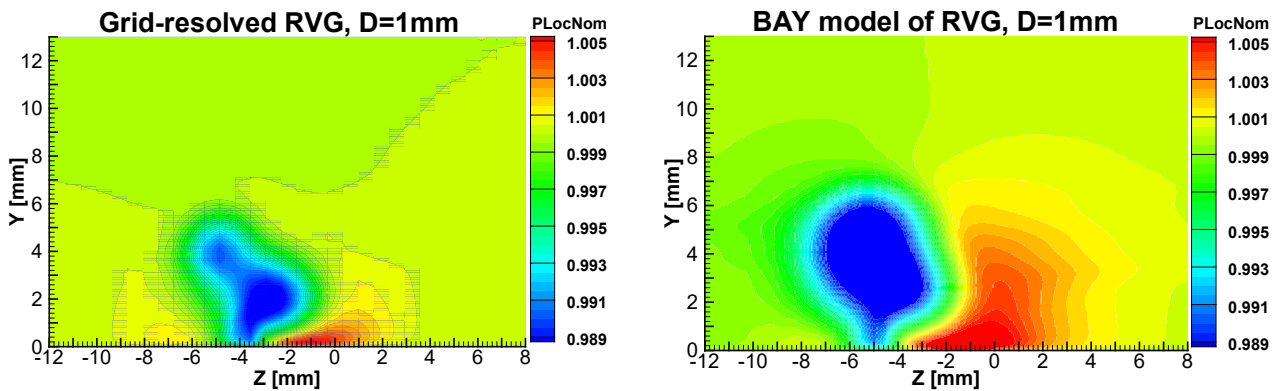*Fig. 7. Normalised local total pressure contour at X = 4.6 cm behind grid-resolved RVG in the left plot and its BAY model in the right plot, diameter D = 1 mm*
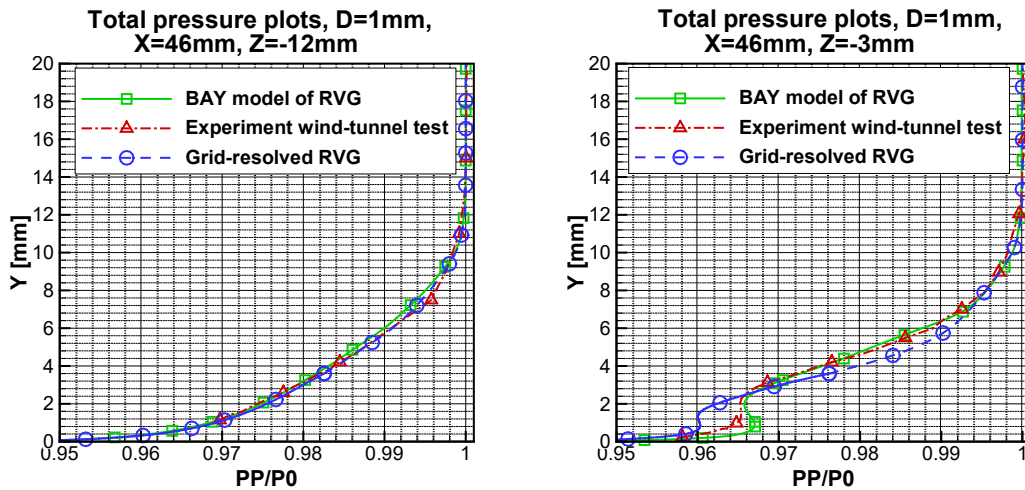

Fig. 8. Plots of total pressure profile in boundary layer in X = 46 mm behind RVG of diameter D = 1 mm for experiment wind-tunnel result, grid-resolved RVG and its BAY model

Additionally, in the case of grid-resolved RVG the region of low pressure has two local minimas, while in experiment there was measured only one. Higher differences between normalised total pressures values in the case of BAY model indicate of higher vortex intensity, which is also accompanied by larger diameter of primary vortex.

In Fig. 8, there are presented plots of total pressure in the boundary layer referenced to the total pressure outside of boundary layer. The total pressure is shown for three cases: measurements (red color with symbols of triangle), grid-resolved RVG (blue colour with symbols of circle) and its BAY

model (yellow colour with symbols of square). In the left plot, it is presented total pressure profile outside of RVG influence on the flow in boundary layer in the spanwise coordinate Z = –12 mm. The very good agreement of plots has been obtained for all cases. In the right plot, it is presented the total pressure profile in the region of influence of RVG in the Z = –3 mm. The character of changes is similar in all cases, where at the height of 1 mm the pressure values are maintained to the height around 2 mm. There is also observed that better agreement with measured total pressure is obtained for BAY model. In the region of momentum transport in the wall-normal direction there is lower total pressure than in the reference case presented in the left plot.

4. Conclusions

BAY model was proposed to predict streamwise vortex generated by rod vortex generator (RVG) of diameter D = 1 mm and height of 3.6 mm placed in the boundary layer of thickness of 10 mm. Firstly, the grid-resolved RVG model was computed using RANS simulation in ANSYS Fluent and then the BAY model was implemented using User Defined Function technique and calibrated using results of circulation downstream grid-resolved RVG model. The mesh of computational domain, where BAY model was applied was coarse and contained only 0.92 millions of cells. The only requirement of mesh for use with BAY model is the size of cells, which must be fine enough to resolve vortices downstream RVG. The results of numerical simulations were compared with measurements at IMP PAN wind tunnel. Despite of the fact, that BAY model constant c_{VG} was calibrated using results of grid-resolved RVG, the better agreement of results with measurements was obtained for results of BAY model. The contours of locally normalized total pressure shown that BAY model better predicted distribution of changes of total pressure in the region of influence of RVG compared with experiment. Proposed modification of BAY model enables to model vortex generators of various dimensions and spatial orientations. Thus, BAY model is a good candidate to predict flows behind RVGs. The BAY model due to its simplicity and low computational cost may be used to find optimal configuration of spatial orientation, diameter and height of RVG. The disadvantage of BAY model is the fact that its constant must be calibrated, in example using experimental data or grid-resolved model computation results.

Acknowledgements

References

[1] Bender, E.E., Anderson, B.H., Yagle, P.J., *Vortex generator modeling for Navier-Stokes codes*, ASME Article FEDSM99-6929, Jul. 1999.
[2] Doerffer, P., Szwaba, R., Flaszyński, P., *PL389685-A1*, 06 June 2011.
[3] Flaszyński, P., *Symulacje numeryczne badań pojedynczego generatora wirów w przepływie poddźwiękowym i naddźwiękowym*, raport IMP PAN, Gdansk 2011.
[4] Flaszyński, P., Szwaba, R., Doerffer, P., *Comparison of vortex generators effect on shock wave induced separation*, AIAA-2016-3328, Conference Proceedings of the (American Institute of Aeronautics and Astronautics) AIAA AVIATION 2016, Washington.

[5] Krzysiak, A., *Zastosowanie nowego rodzaju strumieniowych generatorów wirów do sterowania przepływem*, Prace Instytutu Lotnictwa, Nr 212/2011.

[6] Lin, J.C., *Review of research on low-profile vortex generators to control boundary-layer separation*, Progress in Aerospace Sciences, Vol. 38, pp. 389-420, 2002.

[7] Rokicki, J., Stalewski, W., Żółtak, J., *Evolutionary methods for design, optimization and control*, eds: T. Burczynski and J. Périaux, © CIMNE, Barcelona, Spain 2009.

[8] Stalewski, W., Sznajder,J., *Modification of aerodynamic wing loads by fluidic devices*, Journal of KONES Powertrain and Transport, Vol. 21, No. 3, pp. 271-278, 2014.

[9] Stalewski, W., Sznajder, J., *Computational investigations of active flow control on helicopter-rotor blades*, Journal of KONES Powertrain and Transport, Vol. 21, No. 2, pp. 281-288, 2014.

[10] Szwaba, R., Doerffer, P., *Shock wave boundary layer interaction control by rod vortex generators*, Conference Proceedings of the XXX International Symposium on Shock Waves, Tel Aviv 2015.

[11] Szwaba, R., *Badania eksperymentalne pojedynczych, optymalizowanych, prętowych generatorów wirów w dyszy płaskiej dla M = 0.3*, Opracowanie IMP PAN, Nr arch. 288, Gdansk 2012.

[12] Szwaba, R., *Influence of air-jet vortex generator diameter on separation region*, Journal of Thermal Science, Vol. 22, No. 4, pp. 294-303, 2013.

[13] Sznajder J., Kwiatkowski T., *Effects of turbulence induced by micro vortex generators on shockwave – boundary layer interaction*, Journal of KONES Powertrain and Transport, Vol. 22, No. 2, pp. 241-248, 2015.

[14] Sznajder, J, Kwiatkowski, T., *Selected aspects of introduction of a laminar-flow wing into transport aviation*, Technika Transportu Szynowego Nr 12, 2015.

[15] Tejero, F., Doerffer, P., Szulc, O., *Application of a passive flow control device on helicopter rotor blades*, Journal of the American Helicopter Society, Vol. 61/1, pp. 1-13, 2016.

[16] Tejero, F., Doerffer, P., Flaszyński, P., Szulc, O., *Numerical investigation of rod vortex generators on hovering helicopter rotor blades*, 11th World Congress on Computational Mechanics (WCCM XI), 5th European Conference on Computational Mechanics (ECCM V), 6th European Conference on Computational Fluid Dynamics (ECFD VI), Barcelona, Spain 2014.

[17] Tejero, F., Doerffer, P., Szulc, O., *Aerodynamic analysis of potential use of flow control devices on helicopter rotor blades*, Journal of Physics: Conference Series, 2014, pp. 1-8.